Int J Thermophys (2010) 31:1991–2003
DOI 10.1007/s10765-010-0813-x

Thermal-Conductivity Measurements and Predictions for Ni–Cr Solid Solution Alloys

Rie Endo · Masaya Shima · Masahiro Susa

Abstract Thermal conductivities of Ni–Cr solid solution alloys have been measured to develop a prediction equation for thermal conductivities as functions of temperature and chemical composition. Samples used were Ni–x at% Cr ($0 \leq x \leq 22$) and commercial alloys of Nichrome Nos. 1 and 2. Thermal conductivity measurements were carried out using the transient hot-strip method over a temperature range from 293 K to 1273 K. The thermal conductivities of the alloys increased with increasing temperature and decreased with increasing Cr concentration at constant temperature. The Smith–Palmer equation has been examined to relate the thermal conductivities of the alloys to the electrical resistivities. The thermal conductivity and electrical-resistivity data, respectively, in the present work and in the literature have confirmed that the Smith–Palmer equation applies to Ni–Cr solid solutions and Nichrome alloys. On the basis of this equation, the thermal conductivity of Ni–Cr solid solution alloys has been expressed as a function of temperature and chemical composition. This analysis has also been applied to Ni–Fe and Cu–Ni solid solution alloys.

Keywords Hot-strip method · Ni–Cr · Solid solution alloy · Thermal conductivity

1 Introduction

Many metals and alloys are produced through the molten state at high temperatures. Heat transfer in the processes controls the energy efficiency and the production quality and, hence, optimization of the process parameters. Heat transfer simulation is applied, for which thermophysical properties such as thermal conductivities of molten alloys

---

R. Endo (✉) · M. Shima · M. Susa
Department of Metallurgy and Ceramics Science, Tokyo Institute of Technology,
Ookayama, Meguro-ku, Tokyo 152-8552, Japan
e-mail: rie@mtl.titech.ac.jp

as well as solid alloys are essential as input data. Furthermore, there are numerous practical alloys with a variety of chemical compositions, and thus it is very time-consuming to measure the thermal conductivities of all practical alloys in the molten state. Against this background, it would be useful to develop a prediction equation for thermal conductivities of molten alloys.

On the other hand, most molten alloys are considered to have structures similar to each other, even though they have different chemical compositions. From this structural viewpoint, molten alloys are common with solid solution alloys and, in addition, thermal conductivities of solid solution alloys are much easier to measure. Thus, it would be justified to investigate the development of a prediction equation for thermal conductivities of solid solution alloys, as a first step to a prediction equation for molten alloys, since both equations are expected to take the same mathematical form.

One of the most commonly used prediction methods is based on the Wiedemann–Franz law (W–F law) [1], which is expressed by the following equation:

$$\begin{aligned}\lambda &= L\sigma T\\ &= LT/\rho \qquad (1)\end{aligned}$$

where λ, σ, ρ, T, and L represent the thermal conductivity, electrical conductivity, electrical resistivity, absolute temperature, and Lorenz number, respectively. The electrical conductivity is easier to measure and has a smaller uncertainty than the thermal conductivity, leading to thermal conductivity predictions from Eq. 1. However, when the W–F law is applied to the prediction, the value of L is usually fixed as $2.45 \times 10^{-8}\ \mathrm{W} \cdot \Omega \cdot \mathrm{K}^{-2} (= L_0)$ derived on the basis of the free electron model [1], although real values of L are different from L_0 and have a temperature dependence [2] even in pure metals. One reason for this difference in the Lorenz number is that thermal energy is carried not only by electrons but also by phonons in actual metals, and this difference in L brings about the uncertainty of thermal conductivities calculated from the W–F law.

To relate the thermal conductivity of alloys to their electrical resistivity more reasonably, Smith and Palmer [3] have analyzed thermal conductivities of Cu-based alloys to modify the W–F law as follows:

$$\lambda = AL_0T/\rho + B \qquad (2)$$

where A and B are constants depending on the system. The first term on the right-hand side of Eq. 2 represents the electronic component of thermal conductivity, which comes from the scattering of the electrons by phonons, and follows the W–F law. The second term represents the phonon component of thermal conductivity. The applicability of the Smith–Palmer formula has been reviewed for thermal conductivities of Al-based, Ti-based, and Fe–Cr–Ni alloys by Klemens and Williams [4]; however, it has not been sufficiently analyzed for thermal conductivities of Ni–Cr alloys. This system includes commercial alloys such as Nichrome and Inconel, and, furthermore, is suitable for investigations of the relationship between thermal and electrical conductivities because the alloy system has a wide solid solution region; for example, Cr dissolves into Ni up to about 30 at% at 873 K.

As described above, thermal conductivities of metals and alloys are usually discussed from the viewpoint of electrical resistivities; however, it is also practically important to derive thermal conductivities of alloys from the temperature and chemical composition. Consequently, the present work aims to measure thermal conductivities of Ni–Cr solid solution alloys to develop a prediction equation for thermal conductivities from temperature and chemical composition on the basis of the Smith–Palmer equation.

2 Experimental

2.1 Samples

Samples were Ni–Cr alloys, where the Cr concentrations were (0, 10, 20, and 22) at%. Commercial alloys were also used: Nichrome No. 1 (JIS C2520) and Nichrome No. 2 (JIS C2532) produced by Japan Pure Chemical Co., Ltd. Chemical compositions of the commercial alloys are shown in Table 1. Samples of Ni and the commercial alloys purchased were in a cylindrical shape (30 mm diameter and 40 mm height). Binary alloy samples were prepared from Ni and Cr grains (99.9 mass% purity) using an induction or electric furnace, and machined into a cylindrical shape ((25 to 30) mm diameter and (40 to 50) mm height). Each sample was cut into two parts in the longitudinal direction, and the cut surfaces were polished with a mirror finish. The chemical compositions of the samples were determined by X-ray fluorescence analysis.

2.2 Thermal Conductivity Measurements

The transient hot-strip method was used for the thermal conductivity measurements [5–10]. In this method, an electric current is applied to a thin metal strip (hot strip) placed in the center of the sample, and the temperature rise of the hot strip (ΔT) is recorded continuously. This temperature rise leads to the thermal conductivity of the sample as follows:

$$\lambda = \frac{Q}{4\pi} \Bigg/ \frac{\mathrm{d}\Delta T}{\mathrm{d}\ln t} \tag{3}$$

where Q is the heat generation rate per unit length of the hot strip and t is the time. In practice, ΔT is monitored as the voltage change between two potential wires of the hot strip (ΔV) on the basis of the principle of the four-terminal method, and the value of λ is determined from $\mathrm{d}\Delta V/\mathrm{d}\ln t$ using the following equation [9]:

Table 1 Chemical compositions of commercial alloys in at%

	Ni	Cr	Mn	Si	Fe	C
Nichrome No. 1	74.5	20.6	2.6	1.5	0.1	0.7
Nichrome No. 2	54.4	16.2	1.5	1.5	25.7	0.7

Fig. 1 Conceptual diagram of thermal-conductivity measurement using hot-strip method

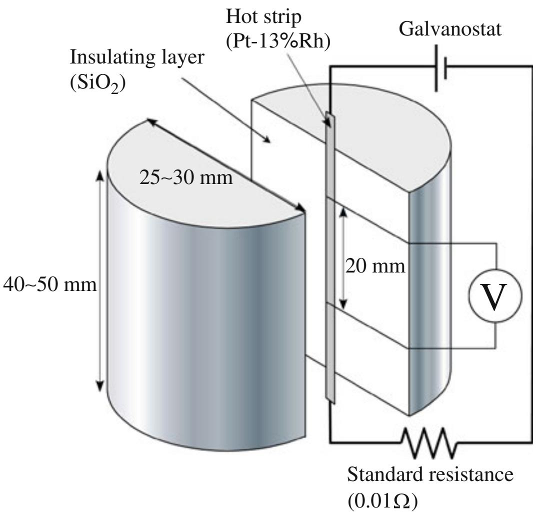

$$\lambda = \frac{I^3 \alpha R_{273} R^{\circ}}{4\pi} \bigg/ \frac{\mathrm{d}\Delta V}{\mathrm{d}\ln t} \tag{4}$$

where I is the current supplied to the hot strip, α is the temperature coefficient of the electrical resistivity of the hot strip at temperature T, R_{273} is the resistance between the potential wires of the hot strip at 273 K, and R° is the resistance per unit length of the hot strip at temperature T. The value of $\mathrm{d}\Delta V/\mathrm{d}\ln t$ is determined from the slope of the linear portion of the relation between ΔV and $\ln t$.

Figure 1 shows a conceptual diagram of the thermal conductivity measurements using the hot-strip method. A hot strip (1 mm width and 0.02 mm thickness) of Pt–13%Rh was sandwiched between two semi-cylindrical samples, which were tightly fixed with a hose clamp. Two platinum potential wires of 0.15 mm diameter were attached to the hot strip spaced apart by about 20 mm to allow four-terminal resistance measurements, and were connected to platinum lead wires of 0.5 mm diameter. This setup enabled the hot strip to serve as a temperature sensor as well. To prevent electrical leakage, the sample surfaces were covered with an insulating SiO_2 film (5 μm thickness) by sputtering. Samples were placed in a flow of Ar–10%H_2 gas in an electric furnace to prevent oxidation during the measurements at high temperature. Measurements were carried out during the heating cycle in the temperature range from 293 K to 1273 K at intervals of about 100 K, and were also carried out during the cooling cycle to confirm the reproducibility of the measurements. Three runs were carried out at each temperature. The current (I = (2.5 to 3.5) A) was supplied to the hot strip via a galvanostat.

3 Results

Figure 2 shows a typical voltage change, ΔV, as a function of the natural logarithm of time, $\ln t$, obtained in measurements on Ni–20 at% Cr at 298 K. It can be seen that there

Fig. 2 ΔV–ln t profile of Ni–20 at% Cr at 298 K

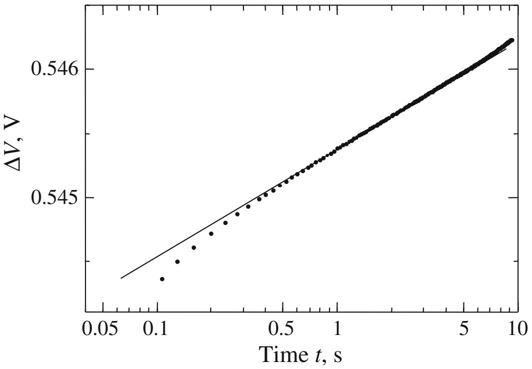

Fig. 3 Thermal conductivities of Ni–Cr solid solution alloys

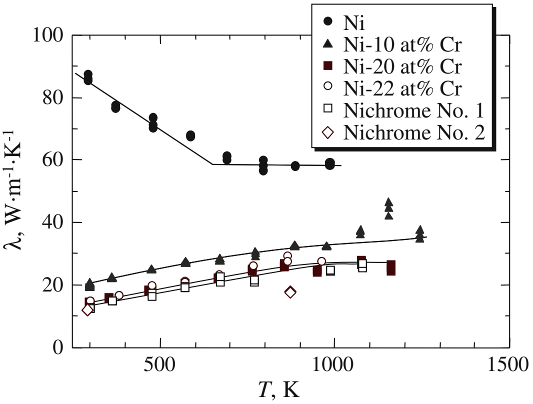

is a linear relation between ΔV and ln$t$ in the time period from 0.5 s to 5 s, and that ΔV deviates from linearity in the time periods below 0.5 s and above 5 s. The former deviation would be due to the effect of the heat capacities of the hot strip and the coating layer, whereas the latter deviation would be due to the effect of heat reflection at the edge of the sample [10,11]. The value of dΔV/dln$t$ has been obtained from the slope of the linear portion and leads to a thermal conductivity of 14.3 W · m^{-1} · K^{-1} from Eq. 4.

Figure 3 shows the temperature dependence of the thermal conductivities of the Ni–Cr and commercial alloy samples obtained in the present work. The thermal conductivity of Ni decreases with increasing temperature up to about 630 K—this temperature would correspond to the Curie point of Ni (631 K), above which the thermal conductivity shows no prominent temperature dependence. This temperature dependence has also been reported by several researchers [12]. The thermal conductivities of Ni–Cr and commercial alloy samples increase with increasing temperature up to about 1000 K and are smaller than that of Ni in the temperature range measured.

Figure 4 shows the temperature dependences of the thermal conductivities of Ni–Cr alloys along with values measured by Shelton et al. [13] and Powell et al. [14], and those calculated from the W–F law using a value of 2.45×10^{-8} W · Ω · K^{-2} for L

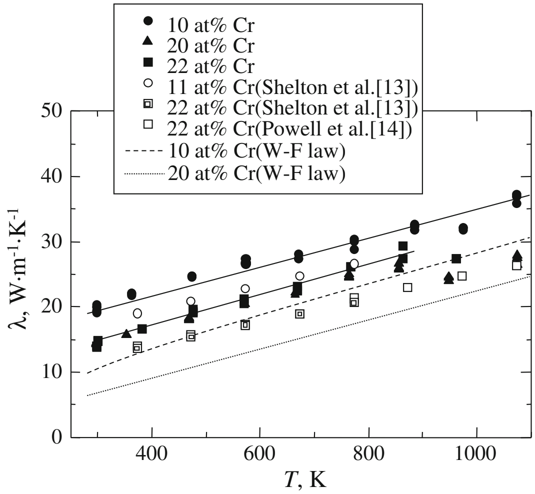

Fig. 4 Thermal conductivities of Ni–Cr solid solution alloys in comparison with reported values

and recommended electrical conductivities [15]. The temperature dependences of the thermal conductivities show good agreement with each other; however, the values in the present work are greater by about 5 $\mathrm{W \cdot m^{-1} \cdot K^{-1}}$ than previously reported values. This difference could be due to measurement methods: for Ni, the reported thermal conductivities range from (30 to 100) $\mathrm{W \cdot m^{-1} \cdot K^{-1}}$ in the literature [12] even at 298 K and the recommended values are 88.5 $\mathrm{W \cdot m^{-1} \cdot K^{-1}}$(273 K to 373 K) [16], 87.8 $\mathrm{W \cdot m^{-1} \cdot K^{-1}}$ (293 K) [17], and 90.5 $\mathrm{W \cdot m^{-1} \cdot K^{-1}}$ (298 K) [18]. The thermal conductivity measured in this study is 86.2 $\mathrm{W \cdot m^{-1} \cdot K^{-1}}$ at 298 K, for which the value is about 3 % smaller than the recommended values; however, the discrepancy would be acceptable for measurements at high temperatures. The values calculated from the W–F law are smaller by about 10 % than those in the present work. This finding indicates that the W–F law cannot be strictly applied to this system, as mentioned in the Sect. 1.

4 Discussion

4.1 Smith–Palmer Plot for Thermal Conductivities of Ni–Cr Solid Solutions

Figure 5 shows the Smith–Palmer plot based on Eq. 2 for the thermal conductivities of Ni–Cr alloy samples including the commercial alloys using recommended electrical-resistivity data [4,15]. Figure 6 shows the electrical-resistivity data for Ni–Cr solid solutions used only [15] for calculations in Fig. 5. There is good linearity between λ and T/ρ, and constants A and B in Eq. 2 have been derived as 0.283 and 10.2 $\mathrm{W \cdot m^{-1} \cdot K^{-1}}$, respectively, by the least-squares method. Consequently, the thermal conductivities can be expressed on the basis of the Smith–Palmer formula as follows:

$$\lambda = 0.283\, L_0 T/\rho + 10.2 \left(\mathrm{W \cdot m^{-1} \cdot K^{-1}}\right) \tag{5}$$

Fig. 5 Smith–Palmer plot for Ni–Cr and Nichrome commercial alloys

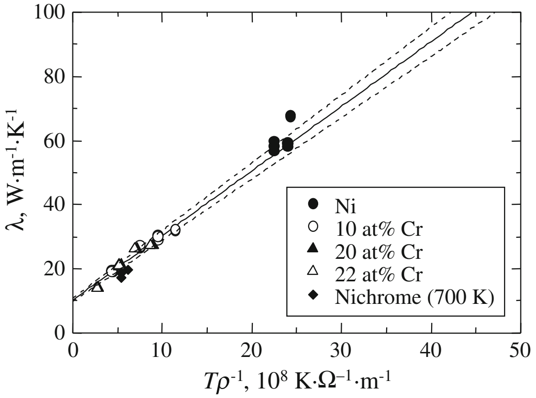

Fig. 6 Electric resistivity of Ni–Cr solid solution alloys as a function of Cr concentration [14]

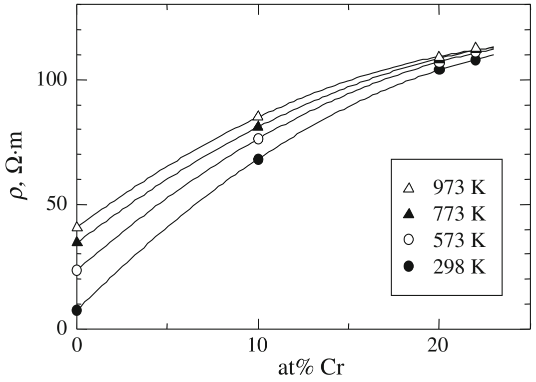

The dashed lines in the figure represent deviations of ±5 % from the regression, which suggests that Eq. 5 can well reproduce the experimental thermal conductivity data. Thus, the Smith–Palmer formula can be applied to thermal conductivities for Ni–Cr solid solution alloys.

4.2 Prediction Equation for Thermal Conductivities of Ni–Cr Solid Solutions as a Function of Temperature and Chemical Composition

Thermal conductivity predictions using the Smith–Palmer formula require electrical-resistivity data, and thus a prediction equation for the thermal conductivity of alloys from temperature and chemical composition would be more useful in practical use. In this part, Eq. 2 is modified into an equation that is a function of temperature and chemical composition only. For this purpose, first, the electrical-resistivity data in Fig. 6 are expressed as a function of temperature and the mole fraction of Cr. Generally, the electrical resistivity of a solid solution is considered as the sum of resistivities due to thermal lattice vibrations (ρ_T) and impurities (ρ_i) as follows:

$$\rho = \rho_T + \rho_i \tag{6}$$

The term ρ_T corresponds to the electrical resistivity of a pure metal and is expressed by the equation $\rho_\mathrm{T} = aT + b$, where a and b are constants; on the other hand, for a binary solid solution, the term ρ_i is related to the mole fraction of the solute component (X) as follows:

$$\rho_\mathrm{i} = D_T X\,(1 - X) \tag{7}$$

where D_T is a temperature-dependent coefficient for the binary system. Equation 7 is known as the original Nordheim rule [19]. Thus, the total electrical resistivity (ρ) is

$$\rho = (aT + b) + D_T X\,(1 - X) \tag{8}$$

This equation is valid when the solute concentration is less than 50 %. To express electrical resistivity for full concentration range, Eq. 8 can be extended as follows [20]:

$$\rho = X\rho_\mathrm{solute} + (1 - X)\,\rho_\mathrm{solvent} + D_T X\,(1 - X) \tag{9}$$

where ρ_solute and ρ_solvent represent the electrical resistivities of the pure solute and solvent metals, respectively. In this study, the concentration of solute, Cr, is less than 50 %, thus, Eq. 8 is applied for further discussion. On the basis of Eq. 8, the electrical resistivities of Ni–Cr solid solution alloys have been regressed to the following equation:

$$\begin{aligned}\rho = {} & (0.0501\,(T - 298) + 8.6178) + (-0.2734\,(T - 298) + 605.12)\\ & \times X_\mathrm{Cr}\,(1 - X_\mathrm{Cr}) \quad \left(10^{-8}\ \Omega\cdot\mathrm{m}\right)\end{aligned} \tag{10}$$

where X_Cr is the mole fraction of Cr; in addition, a reference temperature of 298 K has been used for convenience, and D_T has been approximated as a linear function of temperature. Substitution of Eq. 10 into Eq. 2 enables the thermal conductivity to be predicted from the temperature and the mole fraction of Cr. In the above method, however, electrical-resistivity data for alloys are indispensable to obtain such an expression as Eq. 10.

Second, a prediction equation for the thermal conductivities of Ni–Cr solid solution alloys is formulated using thermal-conductivity data only. Substitution of Eq. 8 into Eq. 2 results in the following equation:

$$\lambda = \frac{AL_0T}{(aT + b) + (cT + d)X(1 - X)} + B \tag{11}$$

where c and d are constants. However, it is very difficult to determine constants A, B, a, b, c and d using thermal-conductivity data only since λ is a complicated function of T and X. For simplicity, Eq. 11 has been approximated using the Maclaurin expansion technique as follows:

Fig. 7 Thermal conductivities of Ni–Cr solid solution alloys as functions of reciprocal of temperature

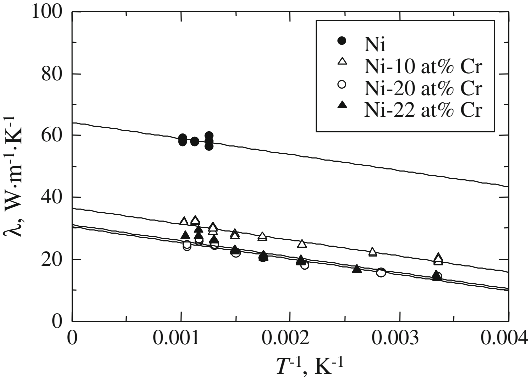

Fig. 8 Reciprocals of intercept of Fig. 6 as a function of $X_{\text{Cr}}(1 - X_{\text{Cr}})$, where X_{Cr} is the mole fraction of Cr

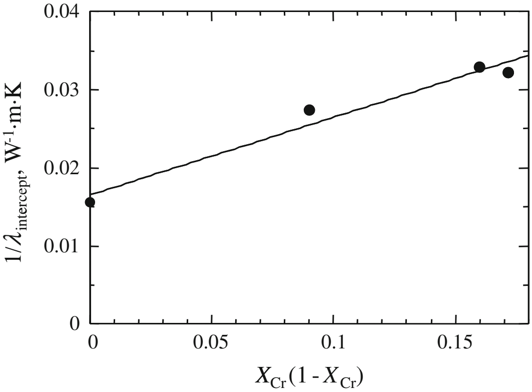

$$\begin{aligned}\lambda &= -\frac{AL_0(b+dY)}{(a+cY)^2}\frac{1}{T} + \frac{AL_0}{a+cY} + B \\ &= AL_0\left(-\frac{b+dY}{(a+cY)^2}\frac{1}{T} + \frac{1}{a+cY} + \frac{B}{AL_0}\right)\end{aligned} \tag{12}$$

where $Y = X(1 - X)$, and the Maclaurin expansion has been made with respect to $1/T$ and $1/Y$.

On the basis of Eq. 12, consider a plot of thermal conductivity versus $1/T$. It is found that there is a linear relationship between thermal conductivity and $1/T$ and that both the slope and intercept of the linear line are functions of Y.

Figure 7 shows the thermal conductivities of Ni–Cr solid solution alloys plotted against $1/T$, where only the data at temperatures above 631 K have been used for Ni because the thermal conductivity of Ni is affected by ferromagnetism below 631 K. It can be seen that there is good linearity between the thermal conductivities and $1/T$ in the alloys and that the slope of each straight line has almost the same value, -5.167×10^3 W · m^{-1}. This finding suggests that the slope is independent of Y, i.e., the mole fraction of Cr within the experimental uncertainty in the composition and temperature ranges investigated. Accordingly, the effect of Cr is reflected only in the intercepts of the straight lines, and consequently, Eq. 12 can be roughly simplified to the following equation:

$$\lambda = \frac{e}{T} + \frac{f}{a + cY} \tag{13}$$

where $e = -5.167 \times 10^3\ \mathrm{W \cdot m^{-1}}$ for Ni–Cr solid solution alloys and f are also constants. Now consider determination of the term $f/(a + cY)$ on the basis of Fig. 7, for which the intercept of the straight line in Fig. 7, corresponding to $f/(a + cY)$, is defined as $\lambda_{\mathrm{intercept}}$, and its reciprocal has been plotted against Y, i.e., $X_{\mathrm{Cr}}(1 - X_{\mathrm{Cr}})$, resulting in Fig. 8. The value of $1/\lambda_{\mathrm{intercept}}$ is linearly proportional to $X_{\mathrm{Cr}}(1 - X_{\mathrm{Cr}})$ and can be regressed to the following equation:

$$1/\lambda_{\mathrm{intercept}} = 0.1055\ X_{\mathrm{Cr}}\ (1 - X_{\mathrm{Cr}}) + 0.0156\ \ (\mathrm{W^{-1} \cdot m \cdot K}) \tag{14}$$

Consequently, using Eqs. 13 and 14, the thermal conductivity of Ni–Cr solid solution alloys has been approximately expressed as a function of temperature and the mole fraction of Cr as follows:

$$\lambda = -5.167 \times 10^3 \frac{1}{T} + \frac{1}{0.1055 X_{\mathrm{Cr}}(1 - X_{\mathrm{Cr}}) + 0.0156}\ \left(\mathrm{W \cdot m^{-1} \cdot K^{-1}}\right) \tag{15}$$

This equation can be applied to the concentration range from (0 to 22) at% Cr. Figure 9 shows the thermal conductivities for Ni–Cr solid solution alloys measured and predicted from Eq. 15, which are represented by symbols and curves, respectively. For Nichrome Nos. 1 and 2, the value of X_{Cr} has been estimated as the sum of mole fractions of all solutes. This figure indicates that there is good agreement between the measured and predicted thermal conductivities, including the commercial alloys. The difference between the measured and predicted thermal conductivities is less than 20 %. Consequently, the thermal conductivities of Ni–Cr solid solution alloys at high temperatures have been described as a function of temperature and the mole fraction of Cr using thermal conductivity data only.

4.3 Applicability of Prediction Equation for Thermal Conductivity to Other Solid Solution Alloys

The applicability of the above analysis to other solid solution systems has also been investigated using thermal conductivity data for Ni–Fe and Cu–Ni systems reported in the literature [21]. Table 2 shows the parameters determined in the same way as described in Sect. 4.2. Figure 10 compares literature and predicted thermal conductivities of Ni–Fe alloys, which are in very good agreement with each other in the temperature range from 800 K to 1200 K and the Fe concentration range from (6.3 to 25) at%. However, there are sufficient discrepancies between the reported and predicted values in the alloys containing less than 4.5 at% Fe and more than 30 at% Fe. The former discrepancy could be due to the compositional dependence of the coefficient of $1/T$, and the latter discrepancy could be due to the possibility that the

Fig. 9 Measured and calculated thermal conductivities for Ni–Cr solid solution alloys

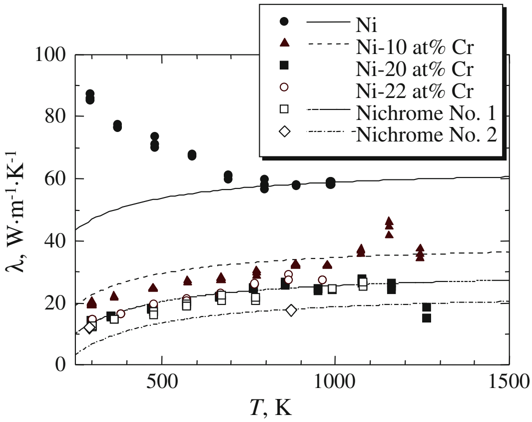

Fig. 10 Thermal conductivities of Ni–Fe system [16] in comparison with predicted values (*solid lines*)

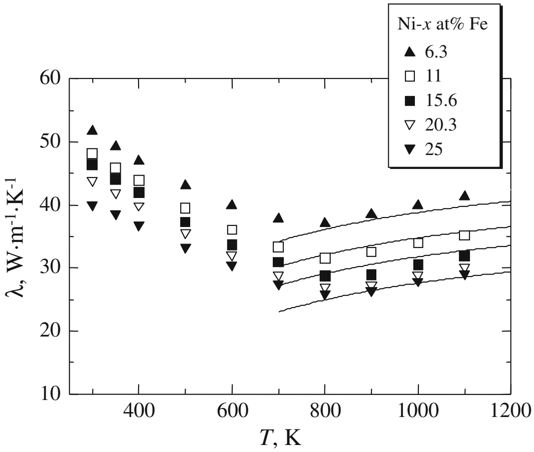

Fig. 11 Thermal conductivities of Cu–Ni system [16] in comparison with predicted values (*solid lines*)

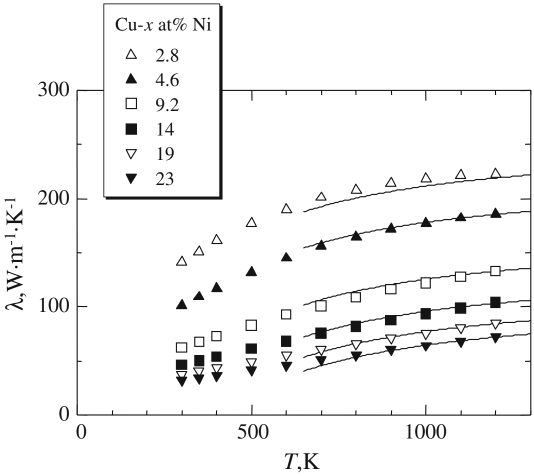

Table 2 Parameters for thermal conductivity prediction: $\lambda = (a + cX(1 - X))^{-1} + eT^{-1}$

System	a ($\mathrm{W^{-1} \cdot m \cdot K}$)	c ($\mathrm{W^{-1} \cdot m \cdot K}$)	e ($10^3\ \mathrm{W \cdot m^{-1}}$)	Conditions
Ni–Cr	0.0156	0.1055	−5.167	$X_{\mathrm{Cr}} < 0.22$
Ni–Fe	0.0175	0.0459	−10.70	$800\,\mathrm{K} < T < 1200\,\mathrm{K}$ $0.045 < X_{\mathrm{Fe}} < 0.3$
Cu–Ni	0.0296	0.0347	−4.440	$700\,\mathrm{K} < T < 1200\,\mathrm{K}$ $0.028 < X_{\mathrm{Ni}} < 0.23$

system is in the two-phase state. Figure 11 compares the thermal conductivities of Cu–Ni alloys measured and predicted, indicating that the prediction equation can be applied to Cu–Ni alloys in the temperature range from 700 K to 1200 K and the Ni concentration range from (2.8 to 23) at%. Figures 10 and 11 suggest that the prediction equation for thermal conductivity proposed in the present work could be applied to liquid alloys as well as other solid solution alloys.

5 Conclusions

The thermal conductivities of Ni–Cr solid solution alloys (Cr concentration ≤ 22 at%) and Nichrome Nos. 1 and 2 alloys have been measured by the hot-strip method in the temperature range from 293 K to 1273 K. The thermal conductivities of Ni–Cr and commercial alloy samples increase with increasing temperature up to 1000 K and are smaller than those of Ni in the measured temperature range. The measured thermal conductivities have been expressed on the basis of the Smith–Palmer equation as follows:

$$\lambda = 0.283 L_0 T/\rho + 10.2 \quad \left(\mathrm{W \cdot m^{-1} \cdot K^{-1}}\right)$$

The prediction equation of thermal conductivities of Ni–Cr alloys has also been formulated as a function of temperature and the mole fraction of Cr as follows:

$$\lambda = -5.167 \times 10^3 \frac{1}{T} + \frac{1}{0.1055 X_{\mathrm{Cr}}(1 - X_{\mathrm{Cr}}) + 0.0156} \quad \left(\mathrm{W \cdot m^{-1} \cdot K^{-1}}\right)$$

This equation could reproduce the thermal conductivities of Ni–Cr solid solution alloys including the commercial alloys, and the difference between the measured and predicted thermal conductivities is less than 20 %. The prediction equation could be extended to other solid solution systems such as Ni–Fe and Cu–Ni alloys.

Acknowledgments The authors would like to express their sincere appreciation to Dr. Amica (Miyamura) Shima of Toshiba Nanoanalysis Co. for valuable discussion as well as instruction about the hot-strip method and to Mr. Kazuki Endo of Mizuho-DL Financial Technology Co., Ltd. for useful suggestions about the mathematical analysis.

References

1. C. Kittel, *Introduction to Solid State Physics*, 7th edn. (John Wiley & Sons, New York, 1998)
2. J.S. Blakemore, *Solid State Physics*, 2nd edn. (W.B. Saunders Company, Philadelphia, 1974)
3. C.S. Smith, E.W. Palmer, Trans. AIME **117**, 225 (1935)
4. P.G. Klemens, R.K. Williams, Int. Metals Rev. **31**, 197 (1986)
5. S.E. Gustafsson, E. Karawacki, N.M. Khan, J. Phys. D: Appl. Phys. **12**, 1411 (1978)
6. S.E. Gustafsson, E. Karawacki, N.M. Khan, J. Appl. Phys. **52**, 2596 (1981)
7. S.E. Gustafsson, J. Appl. Phys. **53**, 6064 (1982)
8. S.E. Gustafsson, E. Karawacki, M.A. Chohan, J. Phys. D: Appl. Phys. **19**, 727 (1986)
9. M. Susa, K. Nagata, K.S. Goto, Trans. Jpn. Inst. Met. **29**, 133 (1988)
10. E. Yamasue, M. Susa, H. Fukuyama, K. Nagata, Metall. Mater. Trans. A **30**, 1971 (1999)
11. E. Yamasue, M. Susa, H. Fukuyama, K. Nagata, J. Cryst. Growth **234**, 121 (2002)
12. Y.S. Touloukian, *Thermal Conductivity: Metallic Elements and Alloys, Thermophysical Properties of Matter* (Plenum, New York, 1970)
13. S.M. Shelton, W.H. Swanger, Trans. Am. Soc. Steel Treat. **21**, 1061 (1993)
14. R.W. Powell, R.P. Tye, Engineer **209**, 729 (1960)
15. A. Goldsmith, T.E. Waterman, H.J. Hirschhorn, *Handbook of Thermophysical Properties of Solid Materials* (Macmillan, New York, 1961)
16. E.A. Brandes, C.J. Smithells, *Smithells Metals Reference Book* (Butterworths, London, 1983), pp. 2–14
17. A. Buch, *Pure Metals Properties: A Scientific-Technical Handbook* (ASM International, Materials Park, OH, 1999), p. 194
18. Japan Society of Thermophysical Properties, *Thermophysical Properties Handbook* (Yokendo, Tokyo, 2008), p. 27
19. R.M. Rose, L.A. Shepard, J. Wulff, *Structure and Properties of Materials: Electronic Properties*, vol. 4 (Wiley, New York, 1966), p. 82
20. G. Lohöfer, J. Brillo, I. Egry, Int. J. Thermophys. **25**, 1535 (2004)
21. P.G. Klemens, G. Klemens, B. Neuer, C. Sundqvist, G.K. Uher, White, in *Landolt-Börnstein, New Series III/15c*, ed. by O. Madelung, G.K. White (Springer, Berlin, 1991)